Spiked-Triangular versus Puckered-Square Geometry in 64-Electron Osmium Clusters. Synthesis and Structure of $Os_4(CO)_{15}(L)$ (L = CO, PF_3, $P(OCH_2)_3CMe$)

Frederick W. B. Einstein,* Victor J. Johnston, and Roland K. Pomeroy*

Department of Chemistry, Simon Fraser University, Burnaby, British Columbia, Canada V5A 1S6

Received February 27, 1990

Clusters of the type $Os_4(CO)_{15}(L)$ have been prepared by the reaction of L with $Os_4(CO)_{14}$ at or below room temperature. The structures of $Os_4(CO)_{16}$ (1), $Os_4(CO)_{15}(PF_3)$ (2), and $Os_4(CO)_{15}[P(OCH_2)_3CMe]$ (3) (the last compound as the CH_2Cl_2 solvate) have been determined by X-ray crystallography: Compound 1 crystallizes in the space group $P\bar{1}$, with a = 9.436 (1) Å, b = 9.482 (1) Å, c = 14.082 (2) Å, α = 87.67 (1)°, β = 79.09 (1)°, γ = 69.69 (1)°, and Z = 2; R_1 = 0.045 and R_2 = 0.054 for 3019 observed reflections. Compound 2 crystallizes in the space group $Pbca$ with a = 15.399 (1) Å, b = 17.757 (2) Å, c = 17.814 (3) Å, and Z = 8; R_1 = 0.046 and R_2 = 0.044 for 2187 observed reflections. Compound 3 crystallizes in the space group $P2_1/c$ with a = 14.220 (2) Å, b = 13.930 (2) Å, c = 17.930 (2) Å, β = 111.65 (1)°, and Z = 4; R_1 = 0.047 and R_2 = 0.050 for 3298 observed reflections. Whereas 1 and 2 have a puckered-square arrangement of metal atoms, 3 has a spiked-triangular metal framework as previously found for $Os_4(CO)_{15}(PMe_3)$ and $Os_4(CO)_{15}(CNBu^t)$; all metal-metal bonds are unbridged. It is concluded that the structure a particular $Os_4(CO)_{15}(L)$ cluster adopts is dictated primarily by the electronic properties of L. The Os–Os bonds in both 1 and 2 are long (they range from 2.977 (2) to 3.005 (2) Å), which suggests they are weak. Consistent with this view is that both 1 and 2 readily decompose in solution at room temperature. The major product in the decomposition of 1 is $Os_3(CO)_{12}$; i.e., $Os_4(CO)_{16}$ is thermodynamically unstable with respect to $Os_3(CO)_{12}$. The stronger metal–metal bonds in $Os_3(CO)_{12}$ are attributed to the occupancy of a molecular orbital that can be considered the result of the overlap of an atomic orbital on each osmium atom directed to the center of the cluster. Because of the long diagonal Os–Os distances in 1 the corresponding overlap is ineffective in 1. In 3, the 18-electron compound $Os(CO)_4[P(OCH_2)_3CMe]$ acts as a donor ligand to the $Os_3(CO)_{11}$ unit via an unbridged, dative metal–metal bond (Os(1)–Os(2) = 2.926 (1) Å). The other Os–Os bond lengths in 3 are 2.849 (1) Å (trans to the dative Os–Os bond), 2.936 (1) Å (cis to the dative Os–Os bond), and 2.882 (1) Å.

Introduction

Most tetranuclear metal carbonyl clusters with 64 valence electrons adopt either the spiked-triangular or square geometry, each with four metal–metal bonds.[1] We have recently described the preparation and structure of $Os_4(CO)_{16}$ (1),[2] $Os_4(CO)_{15}(PMe_3)$ (4),[3] and $Os_4(CO)_{15}(CNBu^t)$ (5).[4] Whereas 4 and 5 have a spiked-triangular metal framework, 1 was unique when first reported in having four unbridged metal–metal bonds in a puckered-square arrangement. Here we describe the synthesis and structure of $Os_4(CO)_{15}(PF_3)$ (2) and $Os_4(CO)_{15}[P(OCH_2)_3CMe]$ (3), along with details of the preparation and structure of 1. From this study and those mentioned above it is concluded that the metal skeleton a particular $Os_4(CO)_{15}(L)$ cluster adopts is dictated primarily by the electronic properties of L.

Experimental Section

Manipulations of starting materials and products were carried out under a nitrogen atmosphere with the use of Schlenk techniques. Hexane was refluxed over potassium, distilled, and stored under nitrogen before use. Dichloromethane was treated similarly, except that P_2O_5 was used as the drying agent. The preparation of $Os_4(CO)_{15}$ has been briefly described;[5] a more detailed description of the synthesis is given here in order that the $Os_4(CO)_{15}(L)$ derivatives described here can be prepared without difficulty. Pentacarbonylosmium[6] and $Os_3(CO)_{10}(COE)_2$ (COE = cyclooctene)[7] were prepared according to literature methods. The ^{13}CO-enriched compounds were obtained from ^{13}CO-enriched $Os_4(CO)_{15}$ prepared from ^{13}CO-enriched $Os_3(CO)_{12}$ (~35% ^{13}C).[3] Group 15 ligands were obtained commercially, except $P(OCH_2)_3CMe$, which was prepared by the method of Heitsch and Verkade.[8] Infrared spectra were recorded on a Perkin-Elmer 983 spectrometer; the internal calibration of the instrument was periodically checked against the known absorption frequencies of gaseous CO. NMR spectra were recorded on a Bruker WM400 spectrometer. Microanalyses were performed by M. K. Yang of the Microanalytical Laboratory of Simon Fraser University.

Preparation of $Os_4(CO)_{15}$. A Schlenk tube was placed in an ice-water bath and charged with $Os_3(CO)_{10}(COE)_2$ (60 mg, 0.057 mmol), CH_2Cl_2 (2 mL), hexane (30 mL) and $Os(CO)_5$ (~20 mg, ~0.06 mmol). The vessel was sealed and placed in a freezer at −15 °C for 4 days; dark red crystals of the product formed. The mother liquor was decanted, and the crystals were washed with hexane and dried on the vacuum line. This afforded analytically pure, crystalline $Os_4(CO)_{15}$ (48 mg, 73%).[5]

Preparation of $Os_4(CO)_{16}$ (1). A 125-mL round-bottom flask fitted with a Teflon valve was charged with $Os_4(CO)_{15}$ (29 mg, 0.025 mmol) and CH_2Cl_2 (35 mL). The solution was degassed by three freeze–pump–thaw cycles. Approximately 1 atm of CO was admitted to the flask and the solution stirred at 0 °C for 4 h. The solvent and excess CO were removed on the vacuum line, and the yellow-orange residue was dissolved in a minimum amount of CH_2Cl_2 and filtered through 1 cm of Celite. Hexane was added to the resulting solution, which was then stored at −15 °C, whereupon $Os_4(CO)_{16}$ (26 mg, 86%) was obtained as air-stable, yellow crystals: IR (hexane) ν(CO) 2075.5 (vs), 2054 (m), 2036.5 (s), 2018.5 (w), 2000 (w), 1993 (sh) cm^{-1}; ^{13}C NMR (CH_2Cl_2/CD_2Cl_2 (5/1), ambient temperature) δ 176.6 and 168.8 (pattern invariant

(1) Sappa, E.; Tiripicchio, A.; Carty, A. J.; Toogood, G. E. *Prog. Inorg. Chem.* **1987**, *35*, 437 and references therein.
(2) Johnston, V. J.; Einstein, F. W. B.; Pomeroy, R. K. *J. Am. Chem. Soc.* **1987**, *109*, 8111.
(3) Martin, L. R.; Einstein, F. W. B.; Pomeroy, R. K. *Organometallics* **1988**, *7*, 294.
(4) Einstein, F. W. B.; Johnston, V. J.; Ma, A. K.; Pomeroy, R. K. *Organometallics* **1990**, *9*, 52.
(5) Johnston, V. J.; Einstein, F. W. B.; Pomeroy, R. K. *J. Am. Chem. Soc.* **1987**, *109*, 7220.
(6) Rushman, P.; van Buuren, G. N.; Shiralian, M.; Pomeroy, R. K. *Organometallics* **1983**, *2*, 693.
(7) Tachikawa, M.; Shapley, J. R. *J. Organomet. Chem.* **1977**, *124*, C19.
(8) Heitsch, C. W.; Verkade, J. G. *Inorg. Chem.* **1962**, *1*, 392.

0276-7333/90/2309-2754$02.50/0

Table I. Summary of Crystal Data and Details of Intensity Collection for $Os_4(CO)_{16}$ (1), $Os_4(CO)_{15}(PF_3)$ (2), and $Os_4(CO)_{15}[P(OCH_2)_3CMe]\cdot CH_2Cl_2$ (3)

	1	2	3
fw	1208.8	1268.9	1414.0
space group	$P\bar{1}$	$Pbca$	$P2_1/c$
cryst syst	triclinic	orthorhombic	monoclinic
a, Å	9.436 (1)	15.399 (1)	14.220 (2)
b, Å	9.482 (1)	17.757 (2)	13.930 (2)
c, Å	14.082 (1)	17.814 (3)	17.930 (2)
α, deg	87.67 (1)		
β, deg	79.09 (1)		111.65 (1)
γ, deg	69.69 (1)		
V, Å^3	1159.9	4870.9	3308.9
Z	2	8	4
ρ_{calcd}, g cm^{-3}	3.46	3.46	2.67
μ(Mo Kα), cm^{-1}	219.42	209.83	154.45
cryst size, mm	0.24 × 0.21 × 0.16	0.21 × 0.18 × 0.11	0.43 × 0.40 × 0.10
scan method	ω–2θ	ω–2θ	ω–2θ
scan range (2θ), deg	2.5–50	2.5–50	2.5–50
scan width (2θ), deg	1.3 + 0.35 tan θ	0.92 + 0.35 tan θ	0.90 + 0.35 tan θ
scan rate (2θ), deg min^{-1}	1.65–2.75	0.92–2.75	0.92–5.49
transmission coeff range	0.211–1.000[a]	0.089–0.213	0.029–0.231
no. of unique rflns	4069	4254	5817
no. of obsd rflns ($I \geq 2.5\sigma(I)$)	3019	2187	3298
no. of variables	166	268	315
R_1[b]	0.045	0.046	0.047
R_2[c]	0.054	0.044	0.050
GOF[d]	1.85	1.10	1.05
largest shift	0.20	0.05	0.20
largest peak, e Å^{-3}	2.8 (4)	1.6 (4)	1.5 (5)

[a] Normalized transmission coefficients. [b] $R_1 = \sum||F_o| - |F_c||/\sum|F_o|$. [c] $R_2 = |\sum w(|F_o| - |F_c|)^2/\sum w|F_o|^2|^{1/2}$. [d] GOF = $[\sum w(|F_o| - |F_c|)^2/(N_{obs} - N_{var})]^{1/2}$.

to −95 °C); a satisfactory MS (EI, FAB) could not be obtained; peaks due to $[Os_3(CO)_{12}]^+$, $[Os_6(CO)_{18}]^+$, etc. were observed in the EI spectrum. Anal. Calcd for $C_{16}O_{16}Os_4$: c, 15.90; H, 0.0. Found: C, 15.89; H, 0.0.

Preparation of $Os_4(CO)_{15}(PF_3)$ (2). A 125-mL round-bottom flask fitted with a Teflon valve was charged with $Os_4(CO)_{15}$ (105 mg, 0.089 mmol) and CH_2Cl_2 (25 mL). The solution was degassed with three freeze–pump–thaw cycles. Approximately 1 atm of PF_3 was admitted to the flask and the solution stirred in a cold bath at −22 ± 5 °C for 30 h. During this period the color of the solution changed from dark green to amber. The solvent and excess PF_3 were removed at −20 °C on the vacuum line, and the orange residue was recrystallized from CH_2Cl_2/hexane (1/1) at −50 °C to yield $Os_4(CO)_{15}(PF_3)$ (22 mg, 20%): IR (CH_2Cl_2) ν(CO) 2125 (w), 2077 (vs), 2067 (s), 2048.5 (s), 2033.5 (s), 2020 (m), 1998.5 (m) cm^{-1}; ^{13}C NMR ($CHFCl_2/CD_2Cl_2$ (6/1), −55 °C) δ 177.0 (2 C, d, J_{P-C} = 10 Hz), 176.5 (4 C), 176.0 (2 C), 169.4 (1 C, br), 169.0 (1 C), 168.8 (1 C), 168.6 (1 C), 168.4 (1 C), 168.0 (1 C), 167.8 (1 C). Anal. Calcd for $C_{15}F_3O_{15}Os_4P$: C, 14.20; H, 0.0. Found: C, 14.25; H, 0.0.

Preparation of $Os_4(CO)_{15}[P(OCH_2)_3CMe]$ (3). A Schlenk tube was charged with $Os_4(CO)_{15}$ (51 mg, 0.043 mmol) dissolved in CH_2Cl_2 (20 mL). The solution was stirred at 0 °C, and a solution of $P(OCH_2)_3CMe$ in CH_2Cl_2 was added dropwise at 5-min intervals. The progress of the reaction was monitored by observing the disappearance of bands due to $Os_4(CO)_{15}$ in the infrared spectrum (the solution turned from dark green to amber during the course of the reaction). When the reaction was judged complete, the solvent was removed at 0 °C on the vacuum line and the yellow residue recrystallized from CH_2Cl_2/hexane at ∼−50 °C to give $Os_4(CO)_{15}[P(OCH_2)_3CMe]$ (21 mg, 37%): IR (CH_2Cl_2) ν(CO) 2116 (w), 2090 (s), 2066 (vs), 2058 (sh), 2051 (s), 2039 (s), 2027.5 (s), 2007.5 (s), 1985.5 (sh), 1960 (sh), 1917 (m, br) cm^{-1}. Anal. Calcd for $C_{20}H_9O_{18}Os_4P$: C, 18.07; H, 0.68. Found: C, 18.32; H, 0.82. The X-ray structure of **3** revealed a molecule of CH_2Cl_2. That this is not indicated in the elemental analysis of **3** can probably be attributed to the thorough drying of the analytical sample.

The $SbPh_3$ derivative $Os_4(CO)_{15}(SbPh_3)$ (**6**) was prepared (37% yield) in a manner similar to that for **3**: IR (CH_2Cl_2) ν(CO) 2118 (w), 2108 (w), 2088 (s), 2069 (w), 2048 (vs), 2032.5 (vs), 2014 (sh) 2004.5 (s), 1975 (m), 1959 (m), 1917 (m, br) cm^{-1}. Anal. Calcd for $C_{33}H_{15}O_{15}Os_4Sb$: C, 25.84; H, 0.99. Found: C, 25.63; H, 1.07.

X-ray Structure Determinations. The following procedure was employed for each of the three structure determinations. Additional details relating to an individual determination are given after the general procedure. A crystal of suitable size (Table I) was mounted, in air, on an Enraf-Nonius CAD4F diffractometer. Diffraction data were collected at 20 ± 1 °C with the use of graphite-monochromated Mo Kα_1 radiation (λ = 0.71069 Å). Background measurements were made by extending the scan range by 25% on each side of the scan. Two standard reflections were monitored every 1 h during data collection, and intensity data were scaled appropriately (in each case the standard reflections varied by less than ±3% during data collection). Lorentz, polarization, and absorption corrections were applied. For **2** and **3** the absorption corrections were analytical corrections that were ψ-scan checked. Accurate cell dimensions were assigned on the basis of 25 carefully centered high-angle ($2\theta > 25°$) reflections that were widely scattered in reciprocal space.

The osmium atoms of **1** and **3** were placed from Patterson maps; those of **2** were placed by direct methods. All other non-hydrogen atoms were located from Fourier difference maps alternated with least-squares refinement. Unit weights were employed initially, but weighting schemes based either on counting statistics (for **1** and **2**) or on an empirical form (for **3**) were adopted during the latter stages of refinement. When counting statistics were used, the weight of a given reflection was determined by $w = [\sigma^2(F) + K(F)^2]^{-1}$ and the value of K adjusted to remove trends in $\langle w(|F_o| - |F_c|)^2\rangle$ in the error analysis. Neutral-atom scattering factors with anomalous dispersion corrections were used.[9] The computer programs used were from "The NRC Vax 750/780 Crystal Structure System"[10a] or the "CRYSTALS"[10b] program suite, except that the thermal ellipsoid diagrams were made with the "SNOOPI" program.[10c] All programs were run on a MicroVAX II computer. Crystallographic data and details of each data collection are given in Table I.

(9) *International Tables for X-ray Crystallography*; Kynoch Press: Birmingham, England, 1974; Vol. IV, Tables 2.2B and 2.3.1.

(10) (a) Gabe, E. J.; Larson, A. C.; Lee, F. L.; Le Page, Y. NRC VAX Crystal Structure System; Chemistry Division, National Research Council: Ottawa, Canada, 1983. (b) Watkin, D. J.; Carruthers, J. R.; Betteridge, P. W. CRYSTALS; Chemical Crystallography Laboratory, University of Oxford: Oxford, England, 1985. (c) Davies, E. K. SNOOPI Plot Program; Chemical Crystallography Laboratory, University of Oxford: Oxford, England, 1985.

Table II. Fractional Coordinates for $Os_4(CO)_{16}$

atom	x/a	y/b	z/c
Os(1)	0.20396 (8)	0.10379 (9)	0.19292 (5)
Os(2)	0.48344 (8)	0.08064	0.27312 (5)
Os(3)	0.32955 (8)	0.39914 (9)	0.34398 (5)
Os(4)	0.09870 (8)	0.43798 (9)	0.21605 (5)
O(11)	0.0534 (16)	0.0797 (17)	0.4049 (10)
O(12)	0.3406 (19)	0.1642 (20)	−0.0140 (11)
O(13)	−0.0800 (23)	0.1096 (23)	0.1201 (13)
O(14)	0.3430 (20)	−0.2346 (21)	0.1629 (12)
O(21)	0.3386	0.0209 (18)	0.4766 (10)
O(22)	0.6043 (16)	0.1638 (17)	0.0692 (9)
O(23)	0.6382 (2)0	−0.2555 (22)	0.2330 (12)
O(24)	0.7665 (18)	0.1052 (18)	0.3344 (10)
O(31)	0.0896 (18)	0.3278 (19)	0.4985 (11)
O(32)	0.5858 (19)	0.4463 (20)	0.1888 (12)
O(33)	0.5187 (22)	0.3381 (22)	0.5021 (13)
O(34)	0.2003 (20)	0.7327 (21)	0.3910 (12)
O(41)	−0.1560 (17)	0.4114 (18)	0.3792 (10)
O(42)	0.3615 (17)	0.4583 (17)	0.0555 (10)
O(43)	−0.0189 (25)	0.772 (3)	0.2418 (15)
O(44)	−0.1018 (19)	0.4442 (20)	0.0705 (11)
C(11)	0.1120 (21)	0.0912 (22)	0.3290 (13)
C(12)	0.2929 (22)	0.1446 (23)	0.0645 (13)
C(13)	0.026 (3)	0.112 (3)	0.1494 (15)
C(14)	0.2908 (23)	−0.109 (3)	0.1761 (13)
C(21)	0.3883 (21)	0.0453 (22)	0.4019 (13)
C(22)	0.5554 (20)	0.1354 (21)	0.1427 (12)
C(23)	0.5766 (24)	−0.128 (3)	0.2454 (14)
C(24)	0.6569 (23)	0.0968 (23)	0.3134 (13)
C(31)	0.1753 (23)	0.3513 (24)	0.4359 (13)
C(32)	0.4926 (24)	0.4231 (25)	0.2434 (14)
C(33)	0.451 (3)	0.360 (3)	0.4382 (15)
C(34)	0.2445 (25)	0.607 (3)	0.3720 (14)
C(41)	−0.0612 (24)	0.4188 (25)	0.3196 (14)
C(42)	0.2737 (22)	0.4438 (23)	0.1160 (13)
C(43)	0.028 (3)	0.643 (3)	0.2376 (17)
C(44)	−0.028 (3)	0.444 (3)	0.1250 (15)

Table III. Selected Molecular Dimensions for $Os_4(CO)_{16}$

Bond Lengths (Å)			
Os(1)–Os(2)	2.997 (1)	Os(1)–Os(4)	2.985 (1)
Os(2)–Os(3)	2.979 (1)	Os(3)–Os(4)	3.000 (1)
Os(1)–C(11)	1.97 (2)	Os(1)–C(12)	1.93 (2)
Os(1)–C(13)	1.87 (2)	Os(1)–C(14)	1.91 (2)
Os(2)–C(21)	1.94 (2)	Os(2)–C(22)	1.95 (2)
Os(2)–C(23)	1.89 (2)	Os(2)–C(24)	1.89 (2)
Os(3)–C(31)	1.92 (2)	Os(3)–C(32)	1.95 (2)
Os(3)–C(33)	1.86 (2)	Os(3)–C(34)	1.88 (2)
Os(4)–C(41)	1.94 (2)	Os(4)–C(42)	1.97 (2)
Os(4)–C(43)	1.84 (2)	Os(4)–C(44)	1.90 (2)
C(11)–O(11)	1.13 (2)	C(12)–O(12)	1.15 (2)
C(13)–O(13)	1.16 (3)	C(14)–O(14)	1.12 (3)
C(21)–O(21)	1.12 (2)	C(22)–O(22)	1.11 (2)
C(23)–O(23)	1.15 (3)	C(24)–O(24)	1.16 (3)
C(31)–O(31)	1.15 (2)	C(32)–O(32)	1.13 (2)
C(33)–O(33)	1.17 (3)	C(34)–O(34)	1.14 (3)
C(41)–O(41)	1.12 (2)	C(42)–O(42)	1.11 (2)
C(43)–O(43)	1.14 (4)	C(44)–O(44)	1.13 (3)
Bond Angles (deg)			
Os(2)–Os(1)–Os(4)	89.22 (3)	Os(1)–Os(2)–Os(3)	88.89 (3)
Os(2)–Os(3)–Os(4)	89.27 (3)	Os(3)–Os(4)–Os(1)	88.73 (3)
Os(2)–Os(1)–C(11)	84.1 (6)	Os(3)–Os(2)–C(21)	81.3 (6)
C(11)–Os(1)–C(12)	171.8 (9)	C(21)–Os(2)–C(22)	173.0 (8)
C(11)–Os(1)–C(13)	92.8 (8)	C(21)–Os(2)–C(23)	91.5 (8)
C(11)–Os(1)–C(14)	92.6 (8)	C(21)–Os(2)–C(24)	93.7 (8)
C(13)–Os(1)–Os(2)	176.6 (6)	C(23)–Os(2)–Os(3)	172.5 (6)
C(13)–Os(1)–C(14)	93.0 (10)	C(23)–Os(2)–C(24)	93.8 (8)
C(31)–Os(3)–Os(4)	81.6 (6)	C(41)–Os(4)–Os(1)	86.2 (7)
C(31)–Os(3)–C(32)	172.9 (9)	C(41)–Os(4)–C(42)	175.2 (8)
C(31)–Os(3)–C(33)	88.5 (9)	C(41)–Os(4)–C(43)	90.6 (10)
C(31)–Os(3)–C(34)	94.7 (9)	C(41)–Os(4)–C(44)	89.7 (9)
C(33)–Os(3)–Os(4)	169.9 (6)	C(43)–Os(4)–Os(1)	176.6 (7)
C(33)–Os(3)–C(34)	94.2 (10)	C(43)–Os(4)–C(44)	95.1 (10)

$Os_4(CO)_{16}$. The data suffered from severe absorption. Several absorption corrections were tried; an empirical correction based on ψ scans gave the best agreement on an isotropic model and was therefore employed in the refinement.[11] The osmium atoms were refined with anisotropic thermal motion parameters, while all other atoms were refined isotropically. Extinction was indicated in the strong, low-angle data and was added as a refinable parameter during the final cycles of refinement. The corrected, calculated structure factor, F_c', was given by the expression $F_c' = K|F_c|(1 + g|F_c|^2 L p_1/p_2)^{1/2}$ and where K is the scale, L is the Lorentz factor, $p_n = 1 + \cos^{2n} 2\theta$, and g is refined to a value of 0.076 (7).[12] In the weighting scheme based on counting statistics $K = 3 \times 10^{-4}$. Final fractional coordinates for the atoms of **1** are given in Table II and bond length and angle data in Table III.

Table IV. Fractional Coordinates for $Os_4(CO)_{15}(PF_3)$

atom	x/a	y/b	z/c
Os(1)	0.27198 (8)	0.39891 (6)	0.01941 (6)
Os(2)	0.44209 (8)	0.32893 (6)	0.06377 (6)
Os(3)	0.37406 (8)	0.30782 (6)	0.21874 (6)
Os(4)	0.24137 (8)	0.42586 (6)	0.18357 (6)
P	0.1430 (7)	0.4377 (5)	−0.0155 (6)
F(1)	0.1219 (17)	0.5196 (12)	−0.0231 (16)
F(2)	0.0631 (15)	0.4148 (16)	0.0256 (18)
F(3)	0.1092 (20)	0.4128 (17)	−0.0865 (17)
O(11)	0.3401 (16)	0.5629 (10)	0.0266 (11)
O(12)	0.3238 (18)	0.3793 (13)	−0.1423 (12)
O(13	0.1984 (14)	0.2373 (11)	0.0296 (11)
O(21)	0.5047 (14)	0.4911 (11)	0.0885 (10)
O(22)	0.6193 (17)	0.2734 (13)	0.1241 (13)
O(23)	0.3691 (15)	0.1674 (10)	0.0443 (10)
O(24)	0.5075 (14)	0.3318 (12)	−0.0977 (12)
O(31)	0.2404 (16)	0.1860 (11)	0.1788 (11)
O(32)	0.3236 (17)	0.2989 (13)	0.3848 (10)
O(33)	0.5080 (15)	0.1814 (10)	0.2335 (12)
O(34)	0.5032 (16)	0.4312 (11)	0.2517 (14)
O(41)	0.2079 (18)	0.4381 (13)	0.3515 (12)
O(42)	0.1020 (14)	0.3045 (11)	0.1630 (13)
O(43)	0.1088 (16)	0.5516 (14)	0.1563 (15)
O(44)	0.3826 (14)	0.5477 (10)	0.1949 (12)
C(11)	0.3158 (19)	0.5024 (15)	0.0257 (15)
C(12)	0.3017 (22)	0.3870 (17)	−0.0784 (20)
C(13)	0.2341 (22)	0.2976 (17)	0.0293 (17)
C(21)	0.4733 (19)	0.4303 (15)	0.0806 (15)
C(22)	0.5527 (22)	0.2934 (16)	0.1002 (17)
C(23)	0.3983 (21)	0.2272 (17)	0.0518 (17)
C(24)	0.4799 (23)	0.3319 (17)	−0.0366 (20)
C(31)	0.2859 (20)	0.2346 (17)	0.1912 (17)
C(32)	0.3378 (19)	0.3028 (14)	0.3202 (16)
C(33)	0.4595 (23)	0.2294 (19)	0.2268 (19)
C(34)	0.4514 (22)	0.3840 (17)	0.2352 (19)
C(41)	0.2202 (20)	0.4348 (15)	0.2879 (17)
C(42)	0.1542 (20)	0.3452 (15)	0.1692 (15)
C(43)	0.1577 (21)	0.5061 (16)	0.1618 (16)
C(44)	0.3345 (20)	0.5021 (15)	0.1902 (15)

$Os_4(CO)_{15}(PF_3)$. Orange crystals of **2** were grown as hexagonal plates from $CHCl_3$/hexane at −50 °C. The orthorhombic space group *Pbca* was chosen after an examination of the systematic absences. After refinement with anisotropic osmium, phosphorus, fluorine, and oxygen atoms, a weighting scheme with $K = 3 \times 10^{-4}$ was adopted for the counting statistics. Final fractional coordinates for the atoms of **2** are listed in Table IV and bond length and angle data in Table V.

$Os_4(CO)_{15}[P(OCH_2)_3CMe]$. Amber, hexagonal plates of **3** were grown from CH_2Cl_2/hexane at ~−50 °C. The monoclinic space group $P2_1/c$ was indicated by the systematic absences. The (100) reflection was found to be in the beam stop and was therefore excluded from the data list. After refinement of all non-hydrogen atoms in **3**, five peaks that were close to one another but were well removed from the positions of the atoms of **3** were found in the difference map. The size and disposition of these peaks were consistent with a disordered molecule of CH_2Cl_2. The best model of the disorder of this molecule consisted of four half-chlorine sites and one full-occupancy carbon site (the occupation factors of these atoms were not refined). Bond length restraints were

(11) North, A. C. T.; Phillips, D. C.; Mathews, F. *Acta Crystallogr., Sect. A: Cryst. Phys., Diffr., Theor. Gen. Crystallogr.* **1968**, *A24*, 351.
(12) Larson, A. C. In *Crystallographic Computing*; Ahmed, F. R., Hall, S. R., Huber, C. P., Eds.; Munksgaard: Copenhagen, 1970.

Table V. Selected Molecular Dimensions for $Os_4(CO)_{15}(PF_3)$

Bond Lengths (Å)			
Os(1)-Os(2)	3.005 (2)	Os(1)-Os(4)	3.000 (2)
Os(2)-Os(3)	2.977 (2)	Os(3)-Os(4)	2.994 (2)
Os(1)-P	2.192 (2)	Os(1)-C(11)	1.96 (3)
Os(1)-C(12)	1.90 (3)	Os(1)-C(13)	1.81 (3)
Os(2)-C(21)	1.89 (3)	Os(2)-C(22)	1.94 (3)
Os(2)-C(23)	1.93 (3)	Os(2)-C(24)	1.88 (3)
Os(3)-C(31)	1.83 (3)	Os(3)-C(32)	1.94 (3)
Os(3)-C(33)	1.96 (3)	Os(3)-C(34)	1.89 (3)
Os(4)-C(41)	1.98 (3)	Os(4)-C(42)	1.98 (3)
Os(4)-C(43)	1.89 (3)	Os(4)-C(44)	1.95 (3)
P-F(1)	1.50 (2)	P-F(2)	1.49 (2)
P-F(3)	1.44 (2)	C(11)-O(11)	1.14 (4)
C(12)-O(12)	1.20 (4)	C(13)-O(13)	1.20 (4)
C(21)-O(21)	1.19 (4)	C(22)-O(22)	1.16 (4)
C(23)-O(23)	1.17 (4)	C(24)-O(24)	1.17 (4)
C(31)-O(31)	1.19 (4)	C(32)-O(32)	1.13 (4)
C(33)-O(33)	1.14 (4)	C(34)-O(34)	1.17 (4)
C(41)-O(41)	1.10 (4)	C(42)-O(42)	1.09 (4)
C(43)-O(43)	1.15 (4)	C(44)-O(44)	1.11 (4)
Bond Angles (deg)			
Os(2)-Os(1)-Os(4)	86.94 (4)	Os(1)-Os(2)-Os(3)	89.38 (4)
Os(2)-Os(3)-Os(4)	87.59 (4)	Os(3)-Os(4)-Os(1)	89.15 (4)
Os(2)-Os(1)-C(11)	94.2 (8)	Os(3)-Os(2)-C(21)	93.6 (8)
C(11)-Os(1)-C(12)	171 (1)	C(21)-Os(2)-C(22)	174 (1)
C(11)-Os(1)-P	92 (1)	C(21)-Os(2)-C(23)	92 (1)
C(11)-Os(1)-C(13)	94 (1)	C(21)-Os(2)-C(24)	93 (1)
P-Os(1)-Os(2)	177.88 (5)	C(23)-Os(2)-Os(3)	88 (1)
C(13)-Os(1)-P	90 (1)	C(23)-Os(2)-C(24)	93 (1)
C(31)-Os(3)-Os(4)	88 (1)	C(41)-Os(4)-Os(1)	93 (1)
C(31)-Os(3)-C(32)	174 (1)	C(41)-Os(4)-C(42)	175 (1)
C(31)-Os(3)-C(33)	95 (1)	C(41)-Os(4)-C(43)	91 (1)
C(31)-Os(31)-C(34)	94 (1)	C(41)-Os(4)-C(44)	90 (1)
C(33)-Os(3)-Os(4)	172 (1)	C(43)-Os(4)-Os(1)	175 (1)
C(33)-Os(3)-C(34)	95 (1)	C(43)-Os(4)-C(44)	91 (1)

employed, and one common isotropic thermal motion parameter was refined for the half-chlorine atoms. There was also evidence for disorder of the $P(OCH_2)_3CMe$ ligand. Several models of the disorder were tried; the best model consisted of anisotropic split oxygen sites (i.e., six oxygen atom sites, each of half-occupancy) and three isotropic carbon sites of full occupancy. The methylene hydrogen atoms were included at calculated positions. Each pair of oxygen atoms of this group were assigned one set of anisotropic thermal motion parameters, and the group was restrained (including vibrational restraints) to meet reasonable geometrical criteria. A Chebyshev[13] weighting scheme was adopted, with the weight given by $w = [12.6216[t_0(x)] + 15.7944[t_1(x)] + 9.22089[t_2(x)] + 1.97702[t_2(x)]]^{-1}$, where $x = |F_o|F_{max}^{-1}$ and t_n are polynomial functions. Final fractional coordinates for all non-hydrogen atoms of **3** are given in Table VI and bond length and angle data in Table VII.

Results and Discussion

Addition of L (L = CO, PF_3, $P(OCH_2)_3CMe$, $SbPh_3$) to $Os_4(CO)_{15}$ in solution at or below 0 °C afforded $Os_4(CO)_{15}(L)$ (eq 1). The binary carbonyl $Os_4(CO)_{16}$ (**1**) was

$$Os_4(CO)_{15} + L \xrightarrow{\leq 0\ ^\circ C} \underset{\textbf{1-3, 6}}{Os_4(CO)_{15}(L)} \qquad (1)$$

L = CO (**1**), PF_3 (**2**), $P(OCH_2)_3CMe$ (**3**), $SbPh_3$ (**6**)

isolated in 87% yield, but yields of the other $Os_4(CO)_{15}(L)$ clusters ranged from 20 to 37%. This is attributed to the low thermal stability of the clusters in solution, especially in the presence of excess L. In the solid state the $Os_4(CO)_{15}(L)$ derivatives are yellow or orange crystalline solids that are reasonably air-stable.

$Os_4(CO)_{16}$ (1). The structure of **1** (Figure 1) shows a puckered-square arrangement of metal atoms. The dihedral angle between the planes Os(1)-Os(2)-Os(3) and Os(1)-Os(3)-Os(4) is 159.9°. The cluster is therefore a

(13) Carruthers, J. R.; Watkin, D. J. *Acta Crystallogr., Sect. A: Cryst. Phys., Diffr., Theor. Gen. Crystallogr.* **1979**, *A35*, 698.

Table VI. Fractional Coordinates for $Os_4(CO)_{15}[P(OCH_2)_3CMe]\cdot CH_2Cl_2$

atom	x/a	y/b	z/c
Os(1)	0.43359 (7)	0.74928 (8)	0.36556 (6)
Os(2)	0.22836 (7)	0.67547 (7)	0.32638 (5)
Os(3)	0.04413 (7)	0.60974 (7)	0.33719 (6)
Os(4)	0.20013 (7)	0.68093 (7)	0.48046 (5)
P	0.5937 (5)	0.8036 (5)	0.3950 (4)
O(1)	0.676 (2)	0.748 (6)	0.460 (7)
O(2)	0.617 (4)	0.904 (5)	0.432 (9)
O(3)	0.630 (4)	0.81 (1)	0.325 (2)
O(10)	0.678 (2)	0.735 (5)	0.443 (8)
O(20)	0.620 (4)	0.900 (6)	0.439 (9)
O(30)	0.622 (4)	0.83 (1)	0.323 (2)
O(11)	0.450 (2)	0.580 (2)	0.260 (1)
O(12)	0.494 (2)	0.613 (2)	0.512 (1)
O(13)	0.378 (1)	0.905 (1)	0.462 (1)
O(14)	0.344 (2)	0.878 (2)	0.216 (1)
O(21)	0.323 (2)	0.475 (1)	0.360 (1)
O(22)	0.155 (1)	0.882 (1)	0.280 (1)
O(23)	0.176 (2)	0.633 (2)	0.152 (1)
O(31)	0.128 (2)	0.404 (1)	0.381 (1)
O(32)	-0.038 (1)	0.814 (2)	0.295 (1)
O(33)	-0.052 (2)	0.562 (2)	0.159 (1)
O(34)	-0.120 (2)	0.564 (1)	0.400 (2)
O(41)	0.304 (2)	0.484 (2)	0.524 (1)
O(42)	0.130 (1)	0.887 (1)	0.439 (1)
O(43)	0.387 (2)	0.765 (2)	0.606 (1)
O(44)	0.065 (2)	0.658 (2)	0.578 (1)
C(1)	0.777 (3)	0.774 (3)	0.472 (3)
C(2)	0.719 (2)	0.937 (2)	0.455 (2)
C(3)	0.727 (2)	0.850 (3)	0.344 (2)
C(4)	0.786 (2)	0.869 (2)	0.433 (1)
C(5)	0.892 (2)	0.902 (2)	0.451 (2)
C(11)	0.444 (2)	0.642 (2)	0.298 (2)
C(12)	0.471 (2)	0.661 (2)	0.456 (2)
C(13)	0.396 (2)	0.847 (2)	0.426 (2)
C(14)	0.373 (2)	0.835 (2)	0.269 (2)
C(21)	0.286 (2)	0.550 (2)	0.351 (2)
C(22)	0.178 (2)	0.805 (2)	0.300 (1)
C(23)	0.198 (2)	0.650 (2)	0.219 (2)
C(31)	0.104 (2)	0.480 (2)	0.365 (2)
C(32)	-0.007 (2)	0.735 (2)	0.311 (2)
C(33)	-0.018 (2)	0.577 (2)	0.226 (2)
C(34)	-0.058 (2)	0.582 (2)	0.375 (2)
C(41)	0.262 (2)	0.553 (2)	0.504 (2)
C(42)	0.153 (2)	0.812 (2)	0.449 (1)
C(43)	0.319 (2)	0.729 (2)	0.558 (2)
C(44)	0.115 (2)	0.664 (2)	0.539 (2)
Cl(1)	0.257 (2)	0.216 (2)	0.325 (2)
Cl(2)	0.427 (2)	0.077 (2)	0.370 (2)
Cl(3)	0.304 (2)	0.082 (2)	0.282 (2)
Cl(4)	0.323 (2)	0.249 (3)	0.357 (2)
C(98)	0.372 (4)	0.166 (4)	0.333 (4)

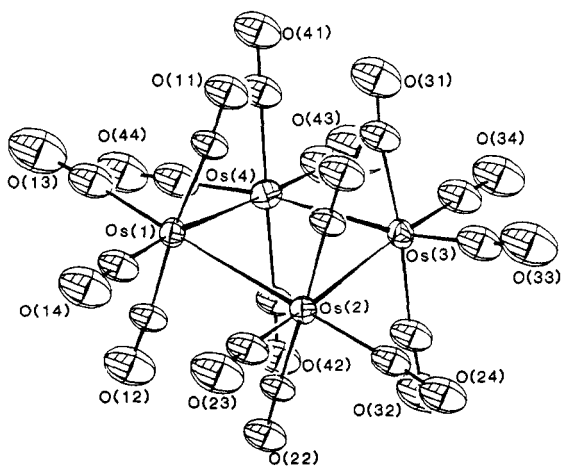

Figure 1. Molecular structure of $Os_4(CO)_{16}$ (**1**).

Table VII. Selected Molecular Dimensions for $Os_4(CO)_{15}[P(OCH_2)_3CMe]$

Bond Lengths (Å)			
Os(1)–Os(2)	2.926 (1)	Os(2)–Os(3)	2.849 (1)
Os(2)–Os(4)	2.936 (1)	Os(3)–Os(4)	2.882 (1)
Os(1)–P	2.269 (6)	Os(1)–C(11)	1.96 (3)
Os(1)–C(12)	1.96 (3)	Os(1)–C(13)	1.94 (3)
Os(1)–C(14)	2.02 (3)	Os(2)–C(21)	1.92 (3)
Os(2)–C(22)	1.94 (3)	Os(2)–C(23)	1.85 (3)
Os(3)–C(31)	1.99 (3)	Os(3)–C(32)	1.88 (3)
Os(3)C(33)	1.91 (3)	Os(3)–C(34)	1.86 (3)
Os(4)–C(41)	1.96 (3)	Os(4)–C(42)	1.96 (3)
Os(4)–C(43)	1.87 (3)	Os(4)–C(44)	1.89 (3)
C(11)–O(11)	1.13 (3)	C(12)–O(12)	1.13 (3)
C(13)–O(13)	1.12 (3)	C(14)–O(14)	1.06 (3)
C(21)–O(21)	1.16 (3)	C(22)–O(22)	1.14 (3)
C(23)–O(23)	1.15 (3)	C(31)–O(31)	1.12 (3)
C(31)–O(31)	1.12 (3)	C(32)–O(32)	1.19 (3)
C(33)–O(33)	1.13 (3)	C(34)–O(34)	1.15 (3)
C(41)–O(41)	1.13 (2)	C(42)–O(42)	1.10 (3)
C(43)–O(43)	1.15 (3)	C(44)–O(44)	1.16 (3)
P–O(1)	1.52 (3)[a]	P–O(2)	1.54 (3)[a]
P–O(3)	1.53 (3)[a]	O(1)–C(1)	1.42 (2)[a]
O(2)–C(2)	1.43 (2)[a]	O(3)–C(3)	1.42 (2)[a]
C(4)–C(1)	1.53 (3)	C(4)–C(2)	1.50 (2)
C(4)–C(3)	1.52 (2)	C(4)–C(5)	1.49 (4)
Bond Angles (deg)			
Os(4)–Os(3)–Os(2)	61.62 (3)	Os(1)–Os(2)–Os(3)	163.31 (4)
Os(1)–Os(2)–Os(4)	103.62 (4)	Os(3)–Os(2)–Os(4)	59.73 (3)
Os(2)–Os(4)–Os(3)	58.64 (3)	P–Os(1)–Os(2)	178.8 (2)
P–Os(1)–C(11)	95.9 (8)	C(11)–Os(1)–C(12)	89 (1)
C(11)–Os(1)–C(13)	169 (1)	C(12)–Os(1)–C(14)	171 (1)
C(21)–Os(2)–C(22)	176 (1)	C(21)–Os(2)–C(23)	89 (1)
C(31)–Os(3)–C(32)	177 (1)	C(31)–Os(3)–C(33)	92 (1)
C(33)–Os(3)–C(34)	102 (1)	C(41)–Os(4)–C(42)	171 (1)
C(41)–Os(4)–C(43)	87 (1)	C(43)–Os(4)–C(44)	103 (1)

[a] Restrained bond length.

metal carbonyl analogue of cyclobutane (the corresponding dihedral angle in C_4H_8 is ~145°).[14] The two fragments $Os(CO)_4$ and CH_2 are, of course, isolobal.[15] This and $Os_4(CO)_{15}(PF_3)$ (**2**), described below, are believed to be the first examples of a metal cluster compound held together by four unbridged metal–metal bonds. Of the clusters reported in the literature, the one that most closely resembles **1** is $[Re_4(\mu_4\text{-}C)(CO)_{15}(I)]^-$. This 64e cluster has a cyclobutane-like metal skeleton held together by a central carbide ligand.[16]

The metal–metal bonds in **1** are remarkably long for Os–Os single bonds; they range from 2.979 (1) to 3.000 (1) Å. The average Os–Os distance of 2.877 (3) Å found in $Os_3(CO)_{12}$ is usually taken as a typial Os–Os single-bond length.[17] The Os–Os bond lengths in noncluster compounds are, however, somewhat longer than this distance. For example, in $Os_3(CO)_{12}(I)_2$ the Os–Os distances are 2.935 (2) Å,[18] in $Os_3(CO)_{10}[P(OMe)_3]_2(Br)_2$ they are 2.916 (1) Å,[19] and in $Os_3(CO)_{12}(SiCl_3)_2$ they are 2.912 (1) Å.[20] Nevertheless, the Os–Os bonds in **1** are still significantly longer than any of these distances.

The torsion angles around the Os–Os bonds are similar for opposite bond pairs: C(11)–Os(1)–Os(2)–C(21) = 6.4 (9)°, C(31)–Os(3)–Os(4)–C(41) = 8.4 (10)°, C(11)–Os(1)–Os(4)–C(41) = 25.6 (9)°, and C(21)–Os(2)–Os(3)–Os(31) = 25.4 (9)°. The Os–Os bonds (Os(1)–Os(2), Os(3)–Os(4)) associated with the smaller torsion angles are slightly longer than those (Os(1)–Os(4), Os(2)–Os(3)) associated with the larger torsion angles (see Table III). These small differences in bond lengths can therefore be attributed to the differences in the interactions of the axial carbonyls associated with each metal–metal bond. The puckered configuration relieves the repulsive interactions between carbonyls syn to each other.

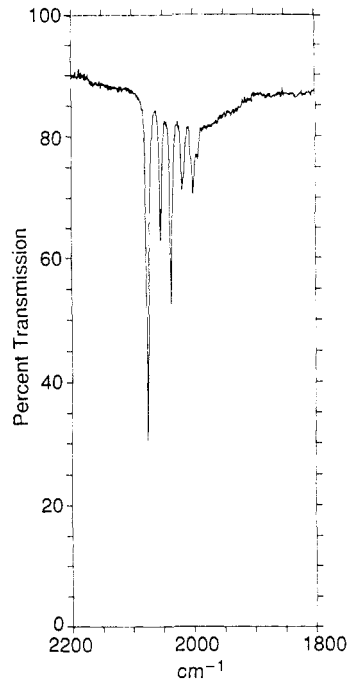

Figure 2. Carbonyl stretching region of the infrared spectrum of **1** in hexane solution.

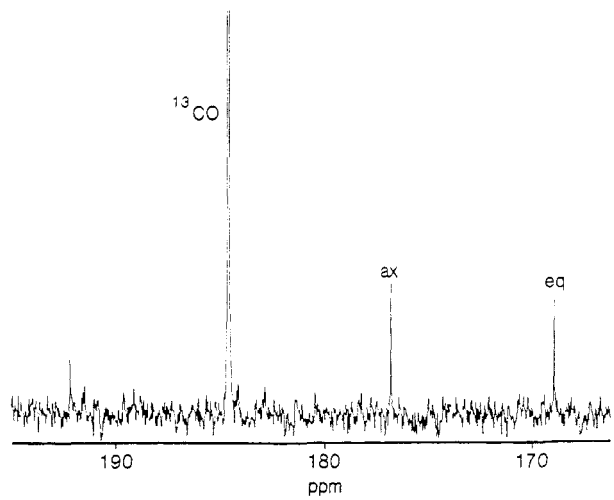

Figure 3. ^{13}C NMR spectrum of the reaction solution of $Os_4(CO)_{15}$ and ^{13}CO in CD_2Cl_2/CH_2Cl_2 after 4 h. The intense peak at δ 184.5 is due to free ^{13}CO.

In hexane, **1** exhibits six infrared-active carbonyl stretches (Figure 2). This is consistent with a puckered (D_{2d}) rather than planar (D_{4h}) configuration in solution as well as in the solid state. The ^{13}C NMR spectrum of **1** (^{13}CO enriched) in CH_2Cl_2/CD_2Cl_2 consists of two resonances at δ 168.8 and 176.6 assigned to the equatorial and axial carbonyls, respectively, by analogy to the spectra of $Os_3(CO)_{11}(L)$ (L = 2e-donor ligand) derivatives.[21-23] Both

(14) Legon, A. C. *Chem. Rev.* **1980**, *80*, 231.
(15) Hoffmann, R. *Angew. Chem., Int. Ed. Engl.* **1982**, *21*, 711.
(16) Beringhelli, T.; Ciani, G.; D'Alfonso, G.; Sironi, A.; Freni, M. *J. Chem. Soc., Chem. Commun.* **1985**, 978.
(17) Churchill, M. R.; DeBoer, B. G. *Inorg. Chem.* **1977**, *16*, 878.
(18) Cook, N.; Smart, L.; Woodward, P. *J. Chem. Soc., Dalton Trans.* **1977**, 1744.
(19) Chen, Y.-S.; Wang, S.-L.; Jacobson, R. A.; Angelici, R. J. *Inorg. Chem.* **1986**, *25*, 1118.
(20) Willis, A. C.; van Buuren, G. N.; Pomeroy, R. K.; Einstein, F. W. B. *Inorg. Chem.* **1983**, *22*, 1162.
(21) (a) Mann, B. E.; Taylor, B. F. *^{13}C NMR Data for Organometallic Compounds*; Academic: New York, 1981; p 176. (b) Aime, S.; Osella, D.; Milone, L.; Rosenberg, E. *J. Organomet. Chem.* **1981**, *213*, 207.

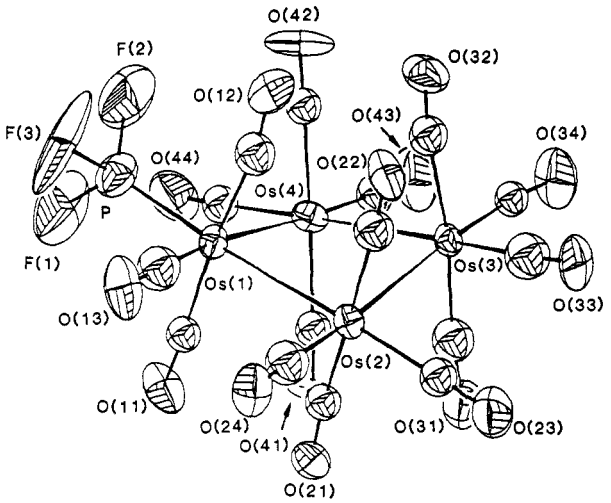

Figure 4. Molecular structure of $Os_4(CO)_{15}(PF_3)$ (2).

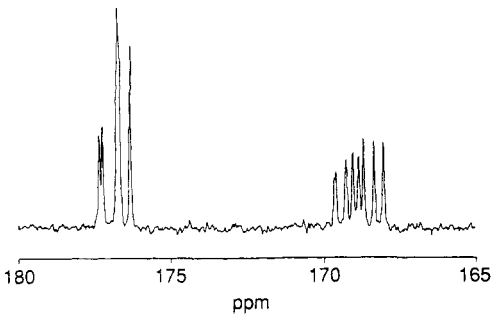

Figure 5. ^{13}C NMR spectrum of 2 in $CHFCl_2CD_2Cl_2$ at −55 °C.

signals remained sharp in the spectrum of 1 at −95 °C, which suggests that there is rapid ring inversion in 1 such that the inner and outer axial carbonyls are rendered equivalent on the NMR time scale. The Os_2C_2 ring in $Os_2(CO)_8(\mu\text{-}C_2H_4)$ exhibits similar behavior.[24]

A CH_2Cl_2/CD_2Cl_2 solution of $Os_4(CO)_{15}$ (with ^{13}CO in natural abundance) was treated with ^{13}CO (99% ^{13}C). A ^{13}C NMR spectrum of the reaction mixture after 4 h showed that both the axial and equatorial sites in the product contained an approximately equal amount of the ^{13}C label (Figure 3). This indicates either that the initial addition of CO to $Os_4(CO)_{15}$ is nonstereospecific or that the addition is stereospecific but that there is axial–equatorial carbonyl exchange in 1 which, although slow on the NMR time scale, is fast on the time scale of the CO-addition experiment. NMR studies of solutions of 1 at higher temperatures, which may have detected axial–equatorial exchange, were precluded by the low thermal stability of the cluster (see below).

$Os_4(CO)_{15}(PF_3)$ (2). The structure of 2 (Figure 4) reveals that it also has a puckered-square arrangement of osmium atoms; the dihedral angle between the Os(1)–Os(2)–Os(3) and Os(1)–Os(3)–Os(4) planes is 151.7°. As in trinuclear carbonyl clusters of osmium, the phosphine occupies an equatorial position.[17,25]

Chart I

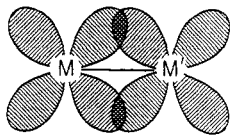

The ^{13}C NMR spectrum of 2 in $CHFCl_2/CD_2Cl_2$ at −55 °C is shown in Figure 5. It consists of seven resonances between δ 167.8 and 169.4 that are assigned to the equatorial carbonyl ligands. Of these resonances, the signal at lowest field (i.e., that at δ 169.4) shows an unresolved coupling to phosphorus. It is probable that this signal is due to the equatorial carbonyl carbon of the $Os(CO)_3(PF_3)$ unit (i.e., C(13)). It is possible, however, that the coupling is a trans, three-bond coupling and therefore the signal is due to C(23). We have found that in $Os_3(CO)_{10}[P(OMe)_3]_2$ trans, three-bond P–P coupling is larger than the corresponding cis two-bond coupling.[23]

The three signals at δ 176.0, 176.5, and 177.0 are assigned to the axial carbonyls with two of the resonances isochronous. The signal at δ 177.0 is a doublet due to phosphorus coupling and can confidently be assigned to the axial carbonyls of the $Os(CO)_3(PF_3)$ grouping. As observed in triosmium clusters,[22,23] the phosphorus–carbon coupling to the axial carbonyls is clearly resolved but that to the equatorial carbonyls is not, even though both are in a position cis to the phosphine ligand. The similarity of the chemical shifts of the ^{13}C signals due to the equatorial and axial carbonyls of 2 to the corresponding resonances of $Os_4(CO)_{16}$ (at δ 168.8 and 176.6, respectively) suggests the electronic effects of the CO and PF_3 are similar in these clusters, a point relevant to the discussion below on the structures of $Os_4(CO)_{15}(L)$ clusters.

The appearance of only four resonances (with two signals degenerate) for the axial carbonyls of 2 is, as discussed for 1, consistent with rapid ring inversion. All the signals remained sharp in the spectrum of 2 with the sample at −120 °C. This indicates the barrier to ring inversion has a low activation energy. The seven sharp signals for the equatorial carbonyls in the spectrum of 2 at −55 °C indicate they do not exchange at this temperature. The variable-temperature ^{13}C NMR spectra of $Os_4(CO)_{15}$ in $CHFCl_2/CD_2Cl_2$ are consistent with an equatorial, merry-go-round CO exchange that is rapid on the NMR time scale even at −120 °C.[26] Such a process in 1 would not be detected by NMR spectroscopy because of the high symmetry of the molecule.

$Os_4(CO)_{15}[P(OCH_2)_3CMe]$ (3). Unlike 1 and 2, the structure of 3 (Figure 6) consists of a spiked-triangular array of metal atoms. The four osmium atoms are essentially planar with Os(1) 0.06 Å from the plane of the osmium triangle. As mentioned in the Introduction, $Os_4(CO)_{15}(PMe_3)$ (4)[3] and $Os_4(CO)_{15}(CNBu^t)$ (5)[4] also adopt spiked-triangular structures. In each case, the 18-electron moiety $Os(CO)_4(L)$ (L = non-carbonyl group) acts as a two-electron-donor ligand to the $Os_3(CO)_{11}$ fragment via an unbridged, dative metal–metal bond.

The length of the dative Os–Os bond in 3 (2.926 (1) Å) is shorter than the corresponding bond in 4 (2.937 (1) and 2.939 (1) Å for the two independent molecules in the unit cell).[3] Although the difference is small, it suggests $Os(CO)_4[P(OCH_2)_3CMe_3]$ is a better donor ligand than $Os(CO)_4(PMe_3)$. This is unexpected, given that PMe_3 is superior to $P(OCH_2)_3CMe$ as a donor ligand.[27] In order to

(22) Johnson, B. F. G.; Lewis, J.; Reichert, B. E.; Schorpp, K. T. *J. Chem. Soc., Dalton Trans.* **1976**, 1403.
(23) Alex, R. F.; Pomeroy, R. K. *Organometallics* **1987**, *6*, 2437.
(24) Motyl, K. M.; Norton, J. R.; Schauer, C. K.; Anderson, O. P. *J. Am. Chem. Soc.* **1982**, *104*, 7325.
(25) For example: (a) Benfield, R. E.; Johnson, B. F. G.; Raithby, P. R.; Sheldrick, G. M. *Acta Crystallogr., Sect. B: Struct. Crystallogr. Cryst. Chem.* **1978**, *B34*, 666. (b) Alex, R. F.; Einstein, F. W. B.; Jones, R. H.; Pomeroy, R. K. *Inorg. Chem.* **1987**, *26*, 3175. See also: Bruce, M. I.; Liddel, M. J.; Hughes, C. A.; Skelton, B. W.; White, A. H. *J. Organomet. Chem.* **1988**, *347*, 157 and references therein.

(26) Einstein, F. W. B.; Johnston, V. J.; Ma, A. K.; Pomeroy, R. K. To be submitted for publication.
(27) Tolman, C. A. *Chem. Rev.* **1977**, *77*, 313.

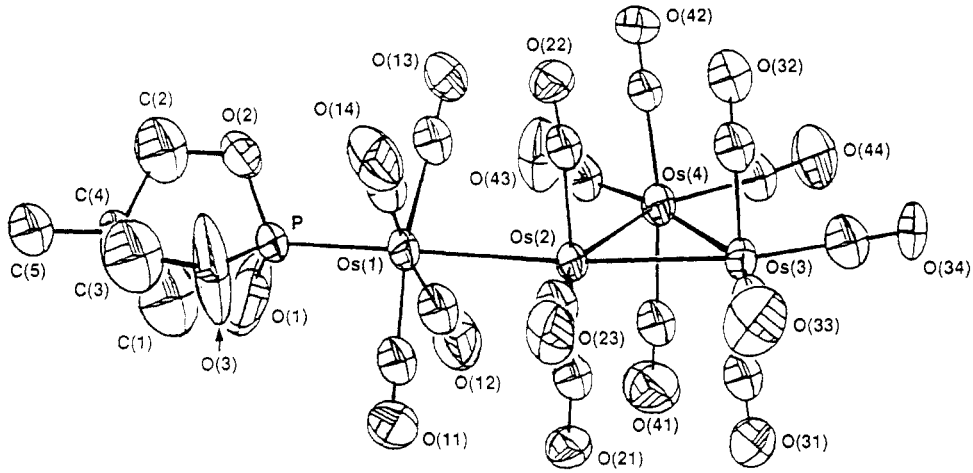

Figure 6. Molecular structure of $Os_4(CO)_{15}[P(OCH_2)_3CMe]$ (3).

explain some of the properties of complexes of the type $(L)(OC)_4OsM(CO)_5$ (M = Cr, Mo, W), we have proposed that there may be a repulsive π-interaction between the filled d orbitals of the metal atoms involved in the dative bond.[28] This is illustrated in Chart I. It may be that the superior π-acceptor properties of the $P(OCH_2)_3CMe$ ligand, compared to those of PMe_3, reduces this interaction when it is trans to the dative metal–metal bond.

The Os–Os bonds within the osmium triangle show significant differences in length (Table VII). A similar variation was found in the Os–Os lengths in **4**[3] and **5**.[4] As previously discussed,[3] the short Os–Os bond trans to the dative Os–Os bond is consistent with the $Os(CO)_4(L)$ ligand being a weak donor ligand.

Comparison of Structures. The cone angles of $P(OCH_2)_3CMe$, PF_3, and PMe_3 are 101, 104, and 118°, respectively.[27] That **3** and **5** have spiked-triangular metal skeletons, whereas **2** has a puckered-square arrangement, cannot therefore be primarily due to the size of the phosphorus ligand. On the other hand, it is well-known that CO and PF_3 have similar electronic properties.[29] Both **1** and **2** have puckered-square metal skeletons. It is therefore concluded that the structure a particular $Os_4(CO)_{15}(L)$ cluster adopts (i.e., spiked triangle or puckered square) is dictated mainly by the electronic properties of L. A deeper understanding of the reasons a particular structure is adopted must await the results of MO calculations. It would be expected, however, that as the σ-donor properties of L increase the dative Os–Os bond would become more stable.[28]

$Os_4(CO)_{15}(SbPh_3)$ (6). In compounds of the type $M'(CO)_4(L)$ (M' = Fe, Ru, Os; L' = group 15 donor ligand), significant amounts of the equatorial isomer are in equilibrium with the axial form for the Ru and Os complexes when L' is an antimony donor ligand. This was attributed to the weak σ-donor property of the Sb ligand, which in these complexes may be weaker than that of CO.[30] For this reason $Os_4(CO)_{15}(SbPh_3)$ (**6**) was prepared by the method shown in eq 1, in order to determine which strucuture it adopts. The pattern of the carbonyl stretches in the infrared spectrum of **6** was the same as that of **4** (Figure 7);[3] that is, the $SbPh_3$ derivative almost certainly adopts the spiked-triangular structure.

It is difficult to draw firm conclusions from this observation. It may be that it is both the σ-donor and π-acceptor properties of L that dictate which configuration a $Os_4(CO)_{15}(L)$ cluster adopts. Alternatively, the puckered-square arrangement may be preferred when L is a weak σ-donor but the spiked-triangular structure is favored when L is a sterically demanding ligand, since in the latter structure the site trans to the spike metal–metal bond is relatively free from steric interactions.

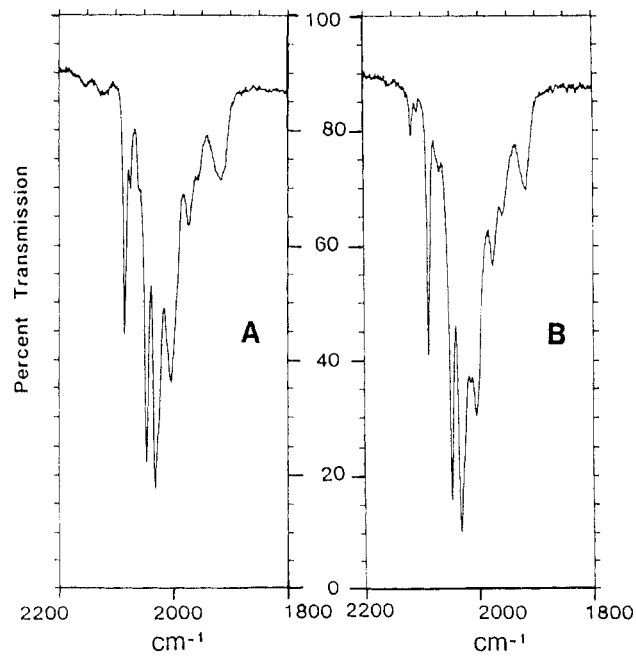

Figure 7. Carbonyl stretching region of the infrared spectra of $Os_4(CO)_{15}(PMe_3)$ (A) and $Os_4(CO)_{15}(SbPh_3)$ (B) in CH_2Cl_2.

Decomposition of 1 (and 2). The long Os–Os bonds in **1** suggest they are weak. This view is supported by the observation that **1** decomposed over 30 h when stirred in hexane, under nitrogen, to give mainly $Os_3(CO)_{12}$ plus a trace of $Os_4(CO)_{15}$ (eq 2). The cluster $Os_4(CO)_{15}$ is stable

$$Os_4(CO)_{16} \rightarrow Os_3(CO)_{12} + Os_4(CO)_{15} \text{ (trace)} \quad (2)$$

in hexane solution at room temperature; therefore, **1** must decompose by different pathways to give $Os_3(CO)_{12}$ and $Os_4(CO)_{15}$.

In the decomposition of $Os_2(CO)_9$ in heptane to give $Os_3(CO)_{12}$, Moss and Graham[31] reported an intermediate with CO stretches at 2077 (m), 2054 (w), and 2000 (w) cm^{-1}. The positions of these bands exactly match those bands

(28) Davis, H. B.; Einstein, F. W. B.; Glavina, P. G.; Jones, T.; Pomeroy, R. K.; Rushman, P. *Organometallics* **1989**, *8*, 1030.
(29) Nixon, J. F. *Adv. Inorg. Chem. Radiochem.* **1985**, *29*, 41.
(30) Martin, L. R.; Einstein, F. W. B.; Pomeroy, R. K. *Inorg. Chem.* **1985**, *24*, 2777.
(31) Moss, J. R.; Graham, W. A. G. *J. Chem. Soc., Dalton Trans.* **1977**, 95.

Chart II

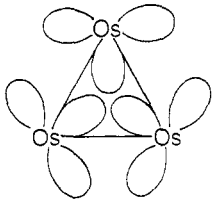

of $Os_4(CO)_{16}$ that would not be obscured by those of $Os_2(CO)_9$ and $Os_3(CO)_{12}$. It therefore appears that 1 is the intermediate in this decomposition and not $Os_2(CO)_8$ as originally suggested. (The unsaturated species $Os_2(CO)_8$ has recently been observed by transient infrared spectroscopy and shown not to have absorptions at these frequencies.[32])

The thermal instability of 1 is in marked contrast to that of $Os_3(CO)_{12}$, which requires temperatures of 210 °C or above to yield products that are the result of Os–Os bond cleavage.[33] The metal–metal bonds in $Os_3(CO)_{12}$ are usually regarded as two-center, two-electron bonds.[34] If this were the case, it might be expected that, even when the increase in the steric interactions of the equatorial carbonyls is taken into account, 1 would be more stable than $Os_3(CO)_{12}$. This is because in 1 the angles about the osmium atoms more closely approach the 90° required for octahedral coordination. But 1 is thermodynamically unstable with respect to $Os_3(CO)_{12}$. We[2] have rationalized this observation that in the trinuclear cluster the most important component of the metal–metal bonding is the occupancy of a molecular orbital located in the center of the metal triangle. Such a molecular orbital can be considered the result of an overlap of an atomic orbital on each osmium atom directed to the middle of the cluster as shown in Chart II. Also in contrast to the case for 1, the syn carbonyls in $Os_3(CO)_{12}$ are eclipsed, an observation that has been taken to indicate that electronic considerations are more important than steric factors in determining the configuration of $Os_3(CO)_{12}$.[35]

There are several theoretical studies that indicate the bonding in trinuclear metal carbonyl clusters should be described in terms of a central molecular orbital, plus edge-bridging molecular orbitals.[36] The longer distance from the osmium atoms to the center of the cluster in 1 compared to that in $Os_3(CO)_{12}$ (~2.11 vs ~1.66 Å, respectively) does not allow for the good overlap of the centrally directed atomic orbitals in 1. The bonding in 1 would therefore be mainly through the edge-bridging molecular orbitals.

Lauher, on the other hand, has argued that weak metal–metal σ-bonds are expected in a square transition-metal cluster due to the angular nodal characteristics of d orbitals.[37] (This phase mismatch does not occur with the p orbitals in cyclobutane). Lauher's treatment, however, assumes the bonding in the metal unit is through the d orbitals with no s,p mixing with these orbitals, which may not be correct.

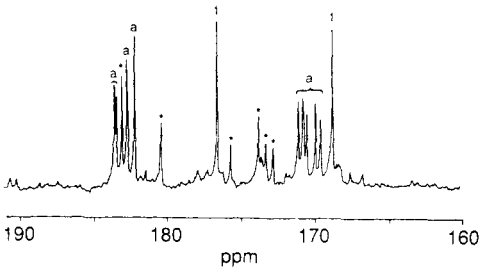

Figure 8. ^{13}C NMR spectrum of the decomposition products of 2 (see text for conditions). The peaks marked 1 are assigned to 1 and those marked with (a) to $Os_3(CO)_{11}(PF_3)$; those with an asterisk are due to an unidentified decomposition product.

Also relevant is the recent theoretical study of the bonding in $Os_2(CO)_8(\mu\text{-}CH_2)$ and $Os_2(CO)_8(\mu\text{-}C_2H_4)$ which revealed that although there are MO's in these complexes that are similar to those in cyclopropane and cyclobutane, respectively, there is an additional MO in each case that is Os–C(ring) antibonding. This interaction arises from the remnants of the t_{2g} orbitals of the $Os(CO)_4$ fragments.[38] Detailed MO calculations on 1 are necessary to determine whether there are similar interactions in 1. Qualitatively, however, it could be envisaged that repulsion between the filled t_{2g}-like d orbitals of the $Os(CO)_4$ units in 1 could be greater than the corresponding repulsions in $Os_3(CO)_{12}$. Again, this arises from the approximately octahedral coordination about the metal atoms in 1. These repulsions are similar to the interaction proposed above for the dative Os–Os bond in 3 and shown in Chart I.

In solution, 2 is less stable than 1. For example, when a hexane/CH_2Cl_2 solution of 2 was stirred under nitrogen at room temperature, it decomposed completely over approximately 4 h. Two of the decomposition products were tentatively identified as $Os_3(CO)_{12}$ and $Os_3(CO)_{11}(PF_3)$ by infrared spectroscopy. However, since many of the CO stretching bands of the products overlapped, this assignment was not definitive. The decomposition was therefore studied by ^{13}C NMR spectroscopy. A ^{13}CO-enriched sample of 2 in CD_2Cl_2/CH_2Cl_2 was allowed to stand at room temperature for 4 h, and then its ^{13}C NMR spectrum was recorded with the sample at −55 °C (Figure 8). The resonances of $Os_3(CO)_{11}(PF_3)$[39] were clearly observed in the spectrum, along with only weak resonances assigned to $Os_3(CO)_{12}$. Surprisingly, the most intense peaks in the spectrum were due to $Os_4(CO)_{16}$ (Figure 8). Given the intensity of these peaks, we do not think that 1 arises from PF_3 dissociation from 2 and then combination of the resulting $Os_4(CO)_{15}$ with adventitious ^{13}CO. A more probable route is that there is initial dissociation of 2 into $Os_3(CO)_8$ and $Os_2(CO)_7(PF_3)$ and 1 results from the combination of two $Os_2(CO)_8$ fragments (i.e., as shown in eq 3).

$$Os_4(CO)_{15}(PF_3) \rightleftharpoons Os_2(CO)_8 + Os_2(CO)_7(PF_3) \quad (3)$$

$$\downarrow \qquad\qquad \downarrow$$

$$Os_4(CO)_{16} \qquad Os_4(CO)_{14}(PF_3)_2$$

Weak signals in the ^{13}C NMR spectrum of the decomposition products may have been due to $Os_3(CO)_{10}(PF_3)_2$

(32) (a) Bogdan, P. L.; Weitz, E. *J. Am. Chem. Soc.* **1990**, *112*, 639. (b) Grevels, F.-W.; Klotzbücher, W. E.; Seils, F.; Schaffner, K.; Takats, J. *J. Am. Chem. Soc.* **1990**, *112*, 1995. (c) Haynes, A.; Poliakoff, M.; Turner, J. J.; Bender, B. R.; Norton, J. R. *J. Organomet. Chem.* **1990**, *383*, 497.

(33) Eady, C. R.; Johnson, B. F. G.; Lewis, J. *J. Chem. Soc., Dalton Trans.* **1975**, 2606.

(34) For example: (a) Cotton, F. A.; Wilkinson, G. *Advanced Inorganic Chemistry*, 4th ed.; Wiley: New York, 1980; p 1083. (b) Wade, K. In *Transition Metal Clusters*; Johnson, B. F. G., Ed.; Wiley: Chicester, England, 1980; p 211. (c) Farrar, D. H.; Goudsmit, R. J. In *Metal Clusters*; Moskovits, M., Ed.; Wiley: New York, 1986; p 41.

(35) Lauher, J. W. *J. Am. Chem. Soc.* **1986**, *108*, 1521.

(36) (a) Lauher, J. W. *J. Am. Chem. Soc.* **1978**, *100*, 5305. (b) Trogler, W. C. *Acc. Chem. Res.* **1990**, *23*, 239 and references therein.

(37) Lauher, J. W. *Int. J. Quantum Chem., Quantum Chem. Symp.* **1988**, *22*, 309.

(38) Bender, B. R.; Bertoncello, R.; Burke, M. R.; Casarin, M.; Granozzi, G.; Norton, J. R.; Takats, J. *Organometallics* **1989**, *8*, 1777.

(39) We have prepared $Os_3(CO)_{11}(PF_3)$ by the reaction of PF_3 with $Os_3(CO)_{11}(CH_3CN)$: Gilmour, B. S.; Wong, E. A.; Ma, A. K.; Pomeroy, R. K. To be submitted for publication.

resulting from the decomposition of $Os_4(CO)_{14}(PF_3)_2$. It would be expected that $Os_4(CO)_{14}(PF_3)_2$ would be less stable than **2**, given that **2** is less stable than **1**.

As we have mentioned above, **1** is apparently an intermediate in the decomposition of $Os_2(CO)_9$ to $Os_3(CO)_{12}$. Further support for the mechanism in eq 3 is that ethylene readily undergoes reversible dissociation from $Os_2(CO)_8(\mu\text{-}C_2H_4)$.[40]

(40) (a) Hembre, R. T.; Scott, C. P.; Norton, J. R. *J. Am. Chem. Soc.* **1987**, *109*, 3468. (b) Takats, J. *Polyhedron* **1988**, *7*, 931.

Acknowledgment. We thank the Natural Sciences and Engineering Research Council of Canada for financial support.

Note Added in Proof. Extended Hückel molecular orbital calculations on **1** have been reported: Mealli, C.; Proserpio, D. M. *J. Am. Chem. Soc.* **1990**, *112*, 5484.

Supplementary Material Available: Tables of hydrogen atom coordinates for **3** and anisotropic thermal parameters for **1**, **2**, and **3** (4 pages); listings of observed and calculated structure factors for **1**, **2**, and **3** (65 pages). Ordering information is given on any current masthead page.

Decomposition of (α-Phenethyl)bis(dimethylglyoximato)cobalt(III) Complexes. Influence of Electronic and Steric Factors on the Kinetics and Thermodynamics of Cobalt–Carbon Bond Dissociation

Flora T. T. Ng,*[1a,b] Garry L. Rempel,[1a,b] Curt Mancuso,[1b] and Jack Halpern*[1b]

Department of Chemistry, The University of Chicago, Chicago, Illinois 60637, and Department of Chemical Engineering, University of Waterloo, Waterloo, Ontario, Canada N2L 3G1

Received March 14, 1990

(α-Phenethyl)bis(dimethylglyoximato)cobalt(III) complexes were found to undergo reversible decomposition reactions according to

$$C_6H_5CH(CH_3)\text{—}Co(DH)_2B \rightleftharpoons Co^{II}(DH)_2B + C_6H_5CH{=}CH_2 + \tfrac{1}{2}H_2$$

which attained measurable equilibria under ca. 1 atm of H_2. The kinetics and, in some cases, equilibria of these reactions were determined for a series of complexes containing different trans-axial ligands B (pyridine (py), 4-CH_3-py, 4-NH_2-py, 4-CN-py, 2-CH_3-py, 2-NH_2-py, imidazole, 2-NH_2CH_2-py, 2-$NH_2CH_2CH_2$-py, aniline, acetone). In the presence of the free-radical trap 2,2,6,6-tetramethylpiperidinyl-1-oxy (Tempo), an additional pathway of decomposition of $C_6H_5CH(CH_3)$–$Co(DH)_2$py was observed that yielded the $C_6H_5\dot{C}H(CH_3)$ radical–Tempo adduct according to

$$C_6H_5CH(CH_3)\text{–}Co(DH)_2py + Tempo \rightarrow Co^{II}(DH)_2py + C_6H_5CH(CH_3)\text{–}Tempo$$

Homolytic Co–C bond dissociation energies, $D_{Co\text{–}C}$, were deduced from measurements of ΔH and $\Delta H^{\ddagger}$ of these reactions and ranged from 17 kcal/mol for B = 2-NH_2-py to 21 kcal/mol for B = 4-NH_2-py. The variations in $D_{Co\text{–}C}$ and in the rates of Co–C bond homolysis were interpreted in terms of the electronic and steric influences of B. Thus, for constant steric influences, $D_{Co\text{–}C}$ increases with the electron-donor ability (pK_a) of B, whereas for constant pK_a, $D_{Co\text{–}C}$ decreases with increasing steric bulk of B. The above reactions proceed through a common rate-determining step, namely, homolysis of the Co–C bond.

Introduction

This paper describes a study of the kinetics and thermodynamics of the Co–C bond dissociation reactions of a series of (α-phenethyl)bis(dimethylglyoximato)cobalt(III) complexes containing different trans-axial ligands. The influences of electronic and steric properties of the latter are examined, along with the influence on the kinetics and product distribution of the free-radical trap 2,2,6,6-tetramethylpiperidinyl-1-oxy (Tempo).

Our studies encompass the determination of the kinetics and equilibrium constants of the reactions depicted by eq 1 (where DH_2 = dimethylglyoxime and B = axial base ligand such as pyridine (py), substituted pyridine, imidazole, aniline, etc.) We have found that certain such reactions (e.g., where B = py, substituted pyridine) attain a readily measurable equilibrium at ambient temperatures under H_2 pressures of ca. 1 atm. The reactions corresponding to the reverse of eq 1 and analogues thereof (including variants involving the addition of "cobalt hydrides" to activated olefins) have previously been recognized as synthetic routes to organocobalt compounds, including organocobalamins.[2-6] The decomposition of other alkylcobalt compounds to yield olefins also is well documented qualitatively.[3,7,8]

$$\underset{\mathbf{1}}{C_6H_5CH(CH_3)\text{—}Co(DH)_2B} = \underset{\mathbf{2}}{Co^{II}(DH)_2B} + C_6H_5CH{=}CH_2 + \tfrac{1}{2}H_2 \quad (1)$$

(1) (a) University of Waterloo. (b) The University of Chicago.

(2) Johnson, A. W.; Mervyn, L.; Shaw, N.; Lester Smith, E. *J. Chem. Soc.* **1963**, 4146.
(3) Schrauzer, G. N.; Windgassen, R. J. *J. Am. Chem. Soc.* **1967**, *89*, 1999.
(4) Schrauzer, G. N.; Holland, R. J. *J. Am. Chem. Soc.* **1971**, *93*, 1505, 4060.
(5) Simandi, L. I.; Szeverenyi, Z.; Budo-Zahoni, E. *Inorg. Nucl. Chem. Lett.* **1975**, *11*, 773.
(6) Simandi, L. I.; Budo-Zahoni, E.; Szeverenyi, Z.; Nemeth, S. *J. Chem. Soc., Dalton Trans.* **1980**, 276.
(7) Schrauzer, G. N.; Sibert, J. W.; Windgassen, R. J. *J. Am. Chem. Soc.* **1968**, *90*, 6681.

0276-7333/90/2309-2762$02.50/0